

Electronic Supplementary Information (ESI)

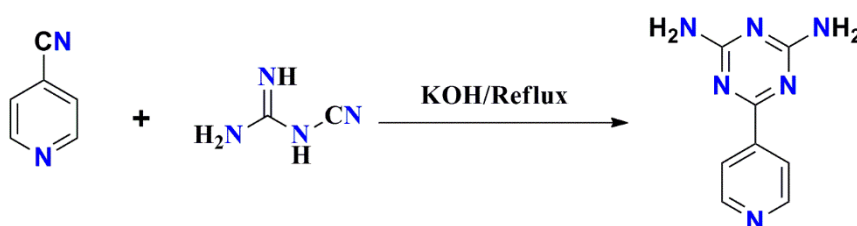
A new set of Cd(II)-coordination polymers with mixed ligand of dicarboxylate and pyridyl substituted diaminotriazine: selective sorption towards CO₂ and cationic dye

Santanu Chand, Syed Meheboob Elahi, Arun Pal, Madhab C. Das*

Department of Chemistry, Indian Institute of Technology Kharagpur 721302, India, Email: mcdas@chem.iitkgp.ernet.in

Ligand Synthesis:

L(NH₂)₂ was synthesized (scheme S1) in a procedure with one step as described below. It has been characterized by ¹H, ¹³C-NMR, Mass (MALDI-TOF), FT-IR and elemental analysis.



Scheme S1: Synthetic scheme for 2,4-diamino-6-(4-pyridyl)-1,3,5triazine): L(NH₂)₂

Procedure for the synthesis of ligand L(NH₂)₂: 4-cyano pyridine (0.707 g, 6.79 mmol) and dicyandiamide (0.832 g, 9.9 mmol) were added to a stirring solution of potassium hydroxide (0.55 g, 9.9 mmol) in 2-methoxy ethanol (20 ml) in a round bottomed flask. The resulting mixture was refluxed at 393K for 30 h. This mixture was subsequently cooled down to room temperature. The solution was neutralized using dilute HCl until the pH of reaction mixture was ~7 to get white precipitate. Then the resulting solution was filtered off, dried under vacuum to get white powder. ¹H NMR (400 MHz, d⁶DMSO, ppm): δ 8.7 (s, 2H), 8.1 (s, 2H), 7.0 (s, 4H); ¹³C NMR (100 MHz, d⁶DMSO, ppm): δ 171, 168, 150, 145, 121; Mass (MALDI-TOF): m/z 189.48 (M+1). Elemental analysis calculated for C₈H₈N₆: C, 51.06%; H, 4.2%; N, 44.6% Found: C, 51.01%; H, 4.5%; N, 43.9%; IR (KBr pellets, cm⁻¹): 3332(m), 3174(m), 2361(m), 2342(m), 1651(s), 1582(s), 1532(s), 1453(s).

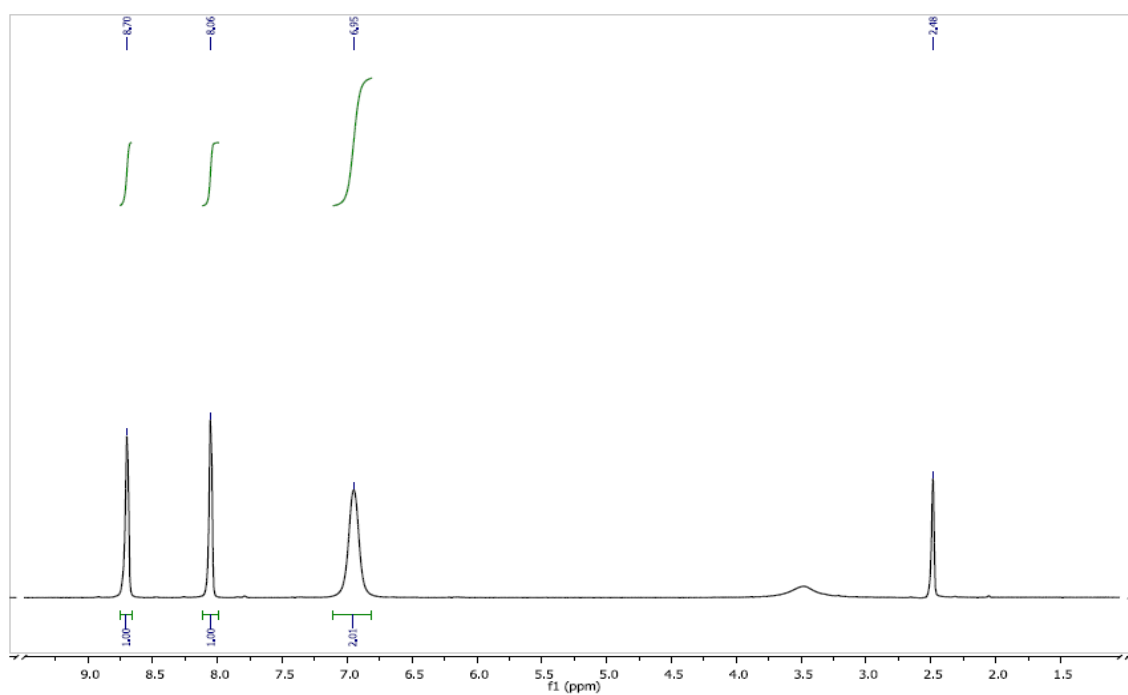


Figure S1: ^1H NMR spectra of $\text{L}(\text{NH}_2)_2$.

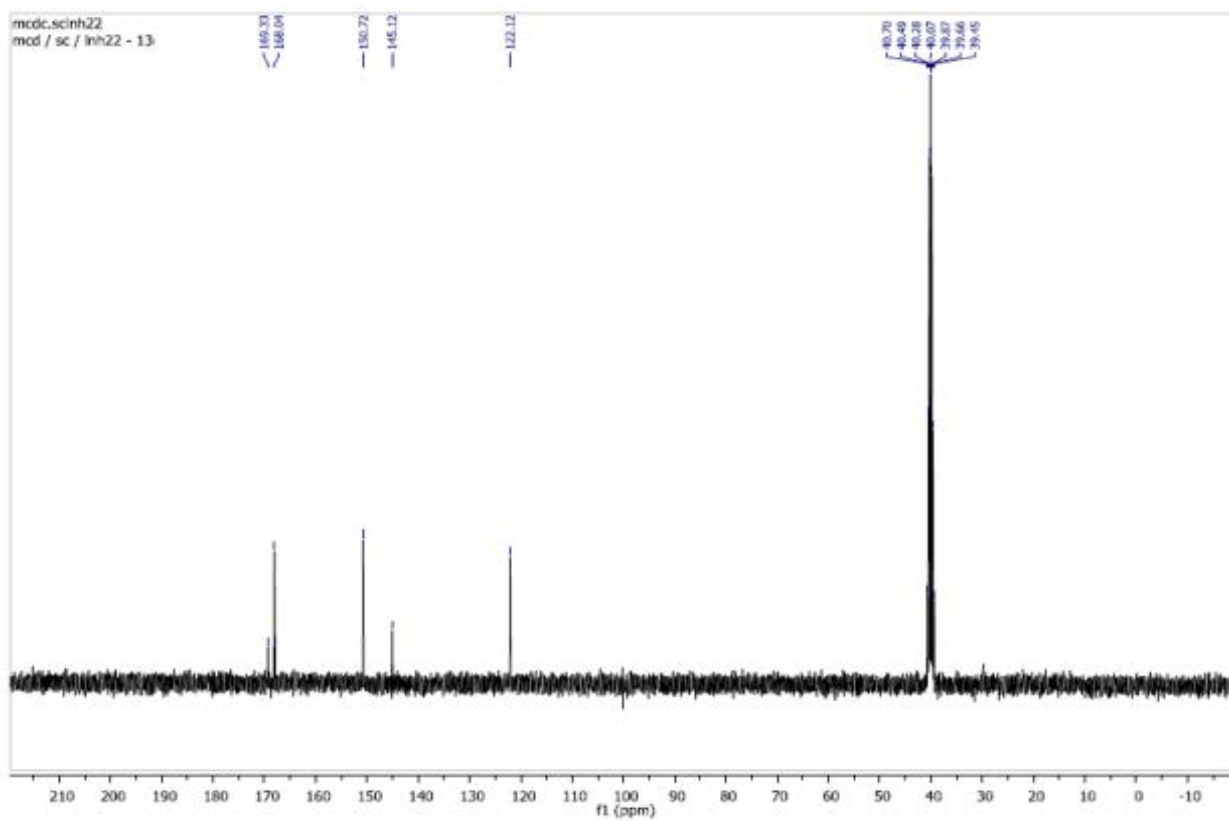
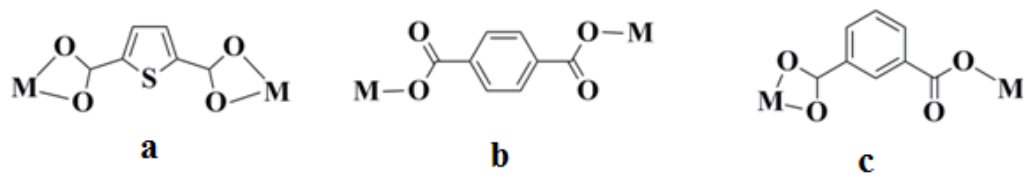
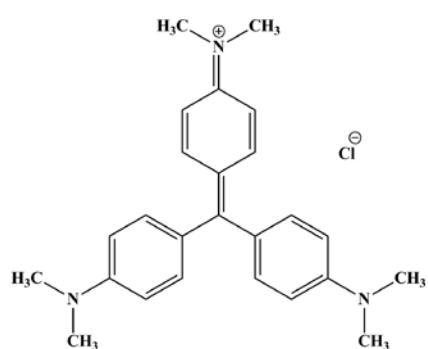


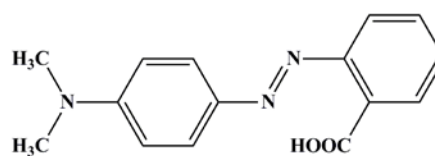
Figure S2: ^{13}C NMR spectra of $\text{L}(\text{NH}_2)_2$.



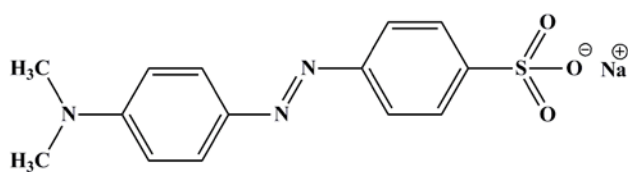
Scheme S2: Bridging modes of the carboxylates.



Crystal Violet



Methyl Red



Methyl Orange

Chart S1: A list of dyes tested for dye adsorption study.

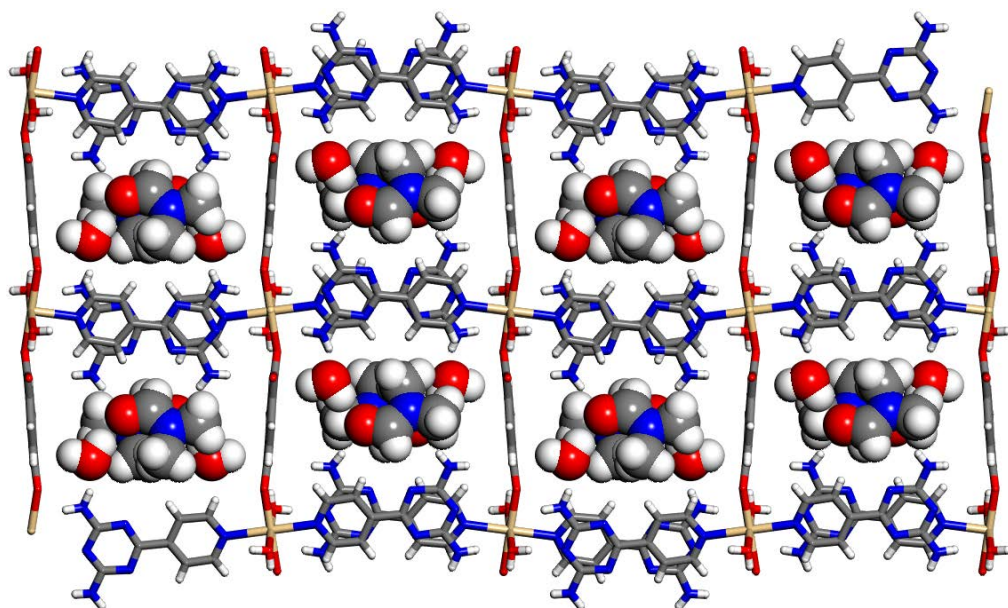


Figure S3: Representation of packing diagram of complex **2** (lattice DMF molecules are shown in space filling model).

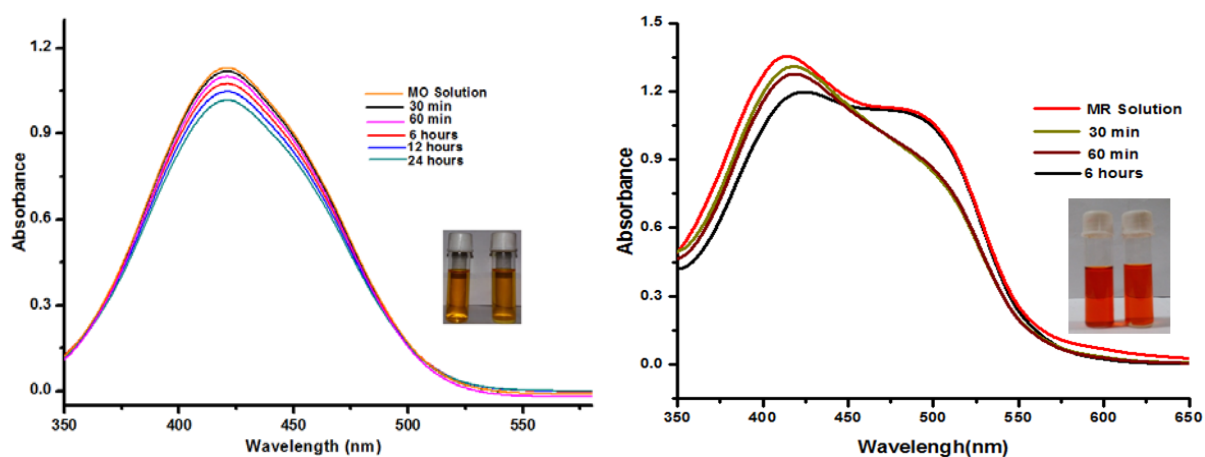


Figure S4: UV–Vis spectra for the uptake of methyl orange (left) and methyl red (right) from methanol solution of **3** at various time intervals.

FTIR Spectra: To check the possible adsorption sites on complex **3**, FT-IR studies have been carried out for **3** (a), crystal violet (b) and crystal violet loaded **3**(c). In the FT-IR spectra of complex **3** (Figure S5) $\nu_{\text{asym}}(\text{NH}_2)$ peak was observed at 3422 cm^{-1} and 3330 cm^{-1} which are red shifted towards lower wave number to 3330 cm^{-1} and 3215 cm^{-1} respectively in crystal violet loaded **3** (c). Another two characteristic peaks $\nu(\text{C=O})$ and $\nu(\text{C=N})$ at 1638 cm^{-1} and 1598 cm^{-1} are also shifted to 1604 cm^{-1} and 1537 cm^{-1} respectively. These shifts may be due to the formation of H-bonding interactions between $-\text{N}(\text{CH}_3)_2^+$ functional groups of the crystal violet and the C=O and free $-\text{NH}_2$ functional groups of complex **3**.

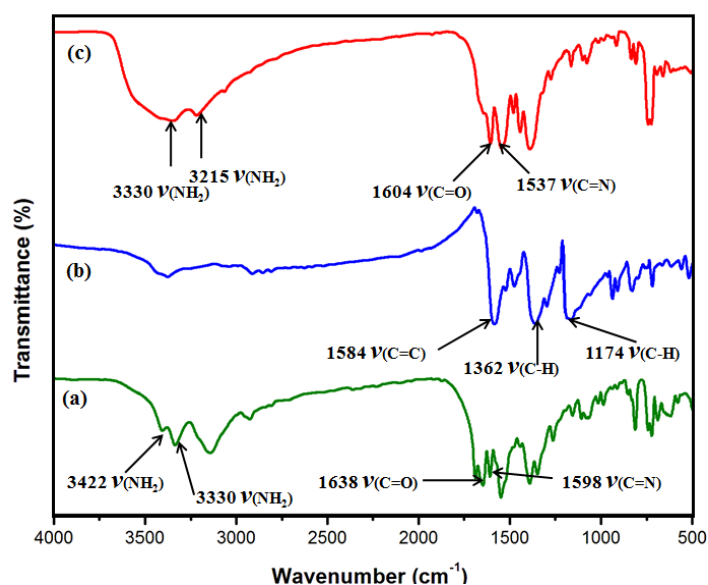


Figure S5: FT-IR spectra of (a) complex **3** (b) crystal violet and (c) crystal violet loaded **3**.

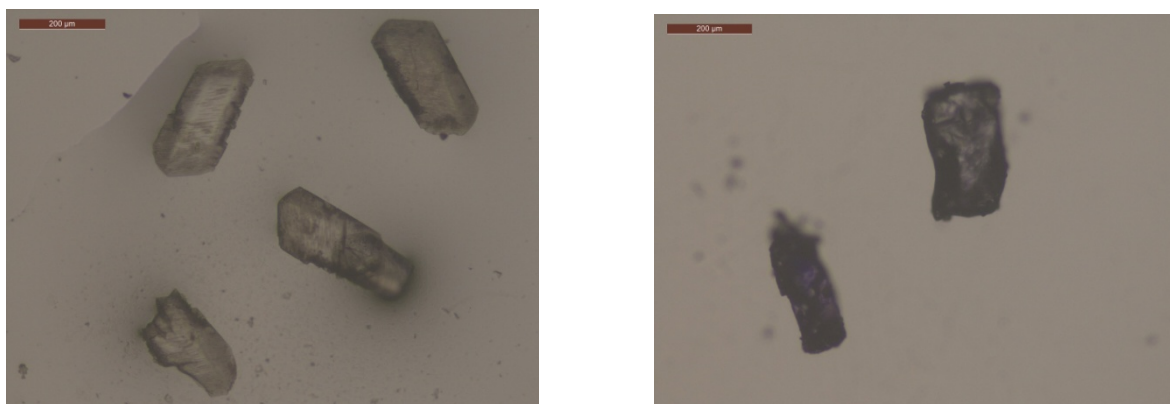


Figure S6: Optical microscopic images (scale: $200\text{ }\mu\text{m}$) of coordination polymer **3** (left) and dye-loaded **3** (right).

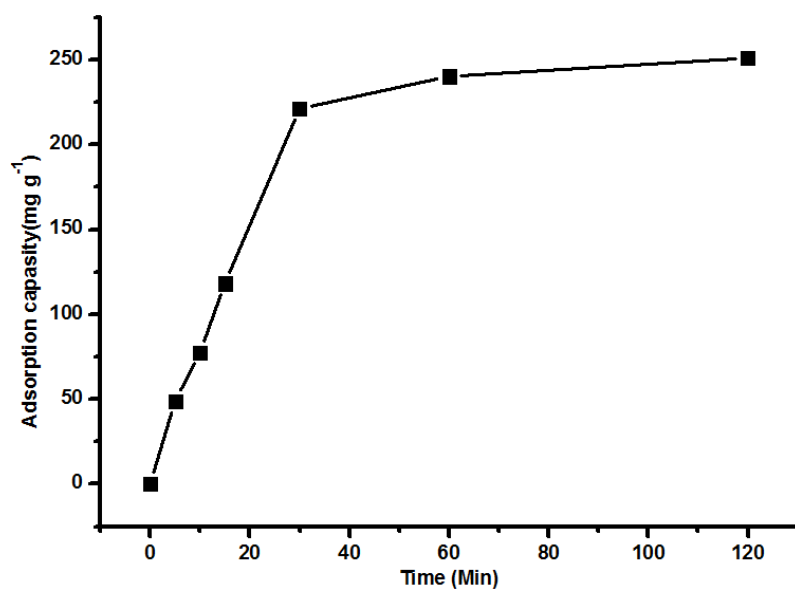


Figure S7: Adsorption capacity of CV as a function of time.

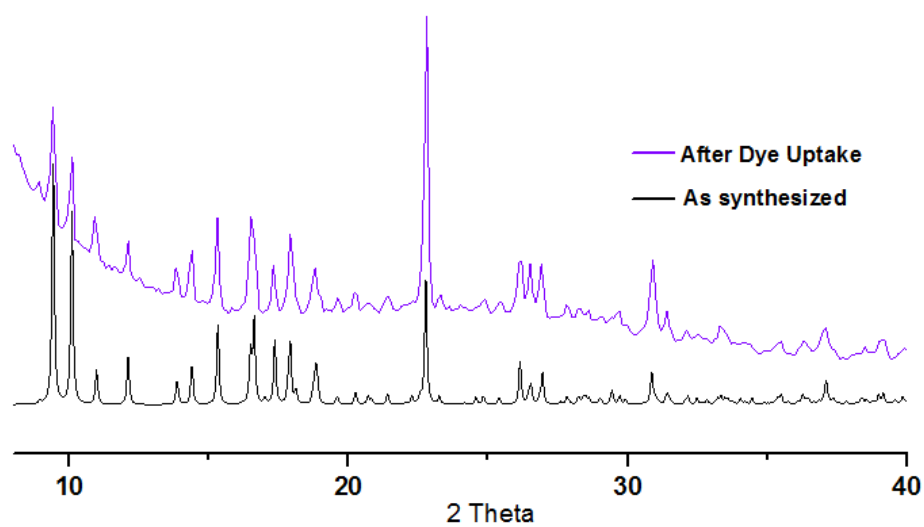


Figure S8: PXRD pattern of **3**, simulated (black) and after dye adsorption (violet).

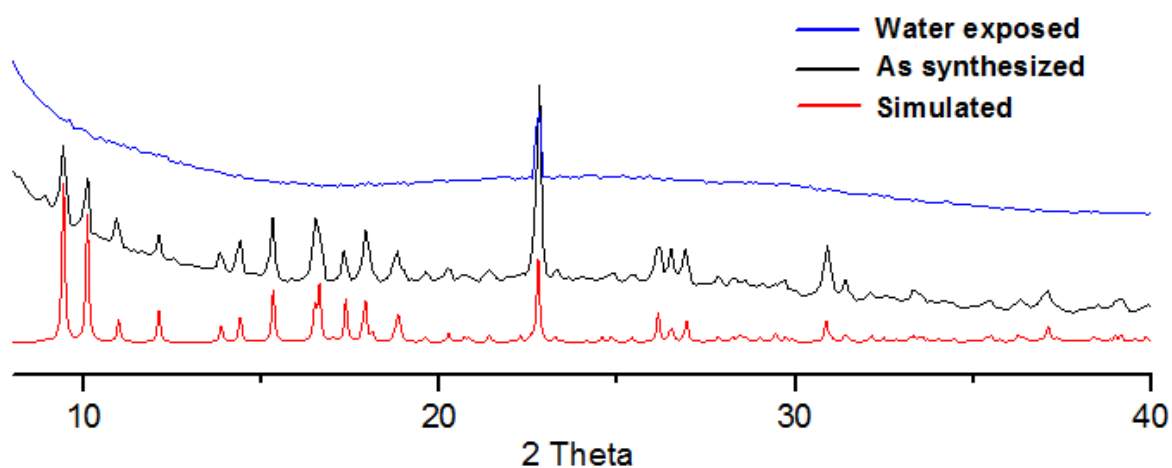


Figure S9: PXRD pattern of **3**, simulated (red), as synthesized (black) and after water exposed for twelve hours.

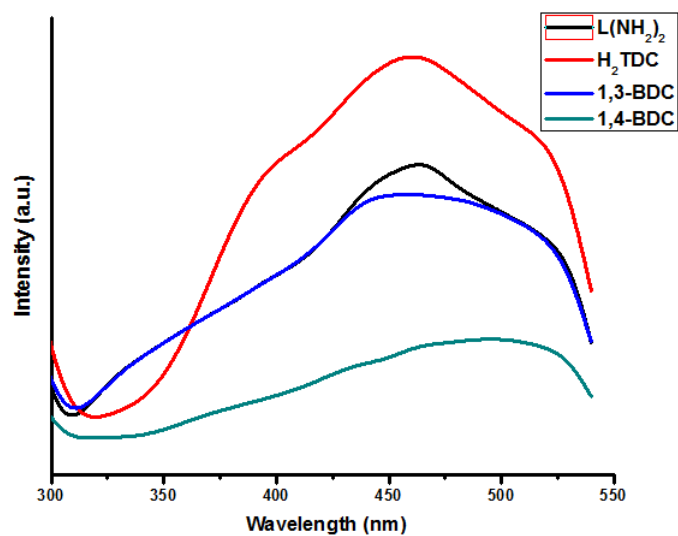


Figure S10. Solid-state photo luminescent spectra of the used ligands.

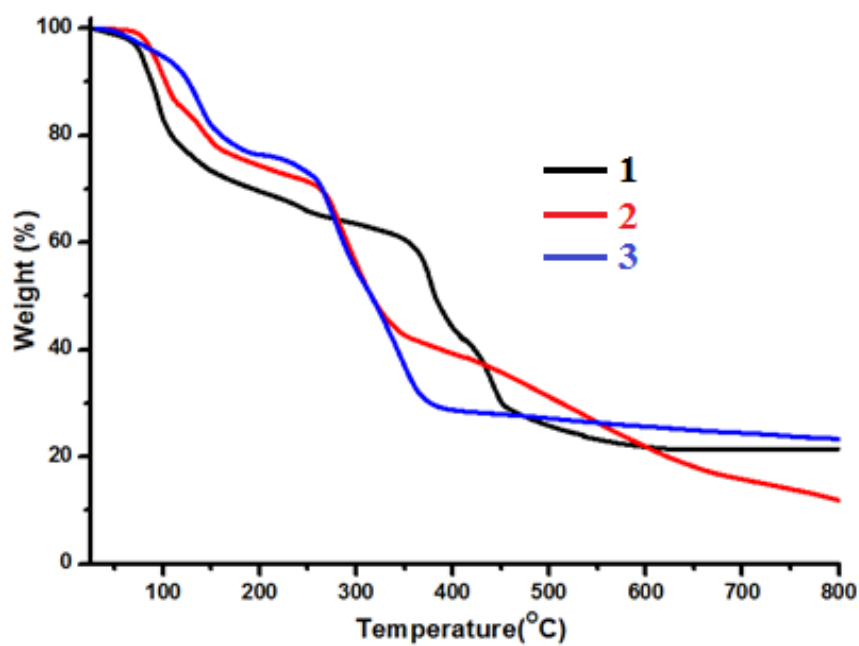


Figure S11: Thermo gravimetric analysis curve of as synthesized complexes **1**(black), **2** (red) and **3** (blue).

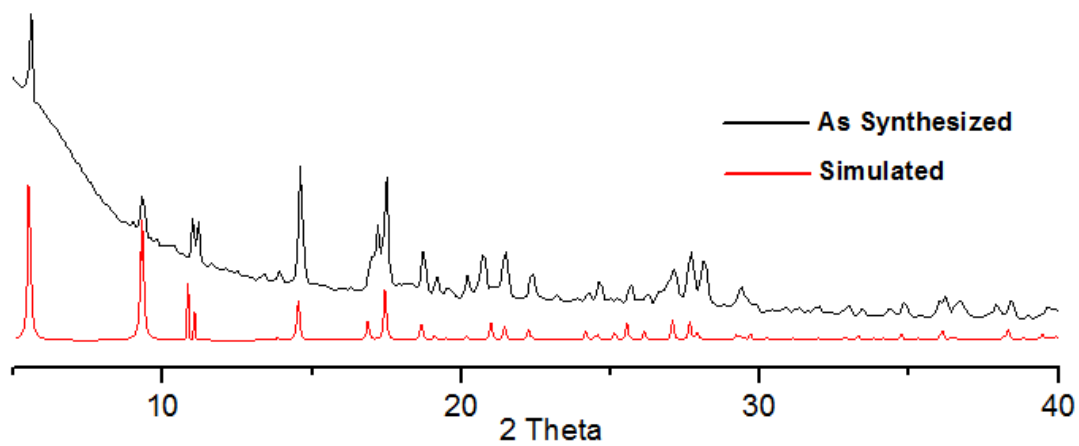


Figure S12: PXRD pattern of complex **1**, simulated (red) and as synthesized (black).

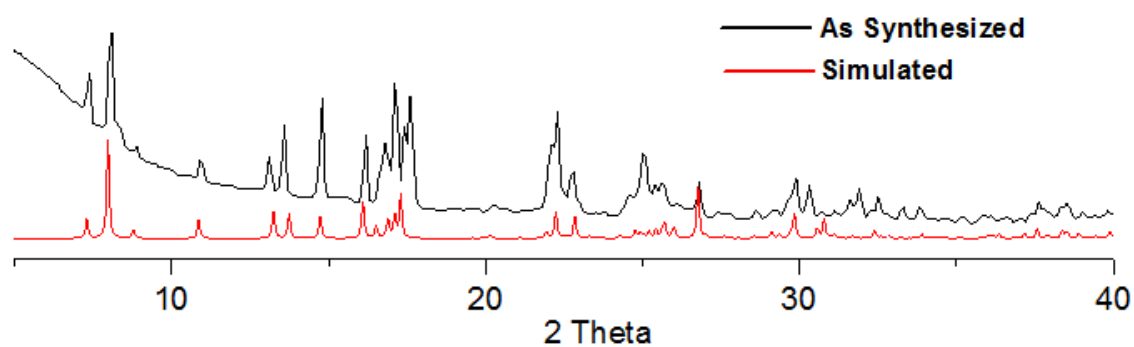


Figure S13: PXRD pattern of complex **2**, simulated (red) and as synthesized (black).

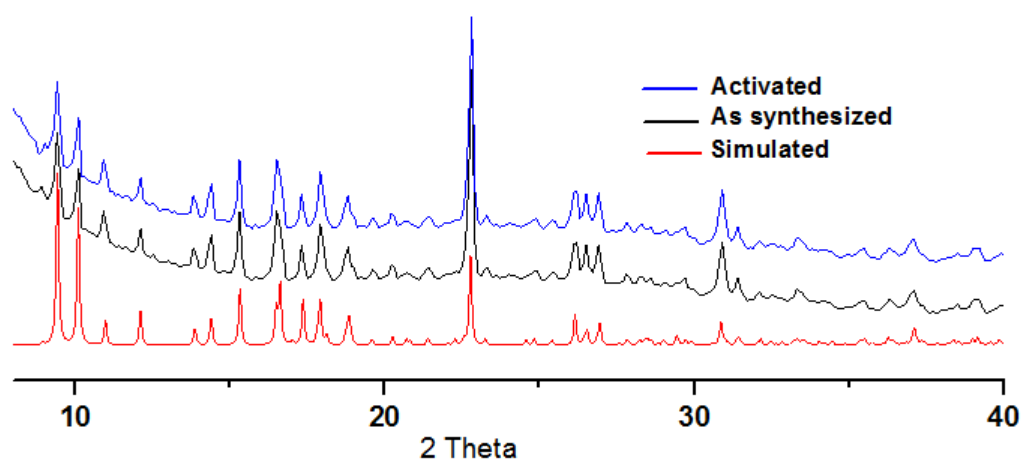


Figure S14: Simulated (red), as synthesized (black) and after activation (blue) PXRD pattern of **3**.

Table S1. Selected bond lengths [Å] and angles [°] for **1-3**.**Complex 1**

Cd1–OW1#1	2.322(2)	Cd1–O2	2.4071(15)
Cd1–OW1#1	2.322(2)	Cd1–O2#1	2.4071(15)
Cd1–N3	2.365(2)	Cd1–O1#1	2.3991(18)
Cd1–O1	2.3991(18)		
#1 -x, y, 1.5-z.			
OW1–Cd1–OW1#1	170.57(9)	OW1#1–Cd1–O2	95.10(7)
OW1–Cd1–N3	85.29(4)	OW1–Cd1–O2	91.74(6)
OW1#1–Cd1–N3	85.29(4)	N3–Cd1–O2	136.47(3)
OW1–Cd1–O1	89.21(8)	O1–Cd1–O2	54.49(5)
OW1#1–Cd1–O1	89.48(8)	O1–Cd1–O2	141.44(5)
N3–Cd1–O1	82.03(4)	O2–Cd1–O2	87.06(7)
OW1#1–Cd1–O1	89.48(8)	OW1#1–Cd1–O2#1	95.10(7)
OW1–Cd1–O1	89.21(8)	OW1–Cd1–O2#1	91.74(6)
N3–Cd1–O1	82.03(4)	OW1–Cd1–O2	95.10(7)
O1–Cd1–O1#1	164.06(8)	N3–Cd1–O2	136.47(3)
OW1–Cd1–O2	91.74(6)	O1#1–Cd1–O2#1	54.49(5)
O1–Cd1–O2	141.44(5)		
#1 -x, y, 1.5-z.			

Complex 2

Cd1–O1	2.2705(18)	Cd1–N1#1	2.3302(2)
Cd1–O1#1	2.2705(18)	Cd1–OW1	2.3578(19)
Cd1–N1	2.3302(2)	Cd1–OW1#1	2.3578(19)
#1 1 -x, -y, 1-z.			

Bond angle:

O1–Cd1–OW1	180	O1–Cd1–OW1#1	87.83(7)
O1–Cd1–N1	91.57(7)	O1#1–Cd1–OW1	92.17(7)
O1–Cd1–N1	88.44(7)	N1–Cd1–OW1#1	89.14(7)
O1–Cd1–N1#1	88.43(7)	N1#1–Cd1–OW1	90.86(7)

O1–Cd1–N1#1	91.57(7)	O4–Cd1–OW1#1	180
N1–Cd1–N1	180.0	N1#1–Cd1–OW1	90.86(7)
O1–Cd1–OW1	92.17(7)	N1–Cd1–OW1	89.14(7)
O1–Cd1–OW1	87.83(7)		

#1 1-x, -y, 1-z.

Complex 3

Cd1–O1	2.223(5)	Cd1–N1	2.353(5)
Cd1–O5	2.280(5)	Cd1–N4	2.467(5)
Cd1–O3	2.349(5)	Cd1–O4	2.426(5)
O1–Cd1–O5	129.2(2)	O1–Cd1–N4	94.24(17)
O1–Cd1–O3	89.09(19)	O5–Cd1–N4	90.98(18)
O5–Cd1–O3	141.23(18)	O3–Cd1–N4	91.97(19)
O1–Cd1–N1	89.65(18)	N1–Cd1–N4	175.81(18)
O5–Cd1–N1	87.75(18)	O4–Cd1–N4	88.09(18)
O3–Cd1–N1	86.54(19)	O3–Cd1–O4	54.86(16)
O1–Cd1–O4	143.94(19)	N1–Cd1–O4	87.85(19)
O5–Cd1–O4	86.64(18)		

Table S2. Non-bonding and H-bonding interactions in complex 1.

D–H...A	d(H...A) (Å)	d(D...A) (Å)	<DHA(°)
C8–H8...OW1	2.683(1)	3.446(2)	139.75(5)
OW1–H2W1...O2	1.890(1)	2.688(1)	175.65(4)
N4–H4A...O1	2.242(1)	2.901(1)	133.32(4)
OW1–H1W1...N1	2.250(1)	3.073(1)	167.82(4)

Table S3. Non-bonding and H-bonding interactions in complex 2.

D–H...A	d(H...A) (Å)	d(D...A) (Å)	<DHA(°)
C12–H15...O2	2.508(1)	3.307(2)	144.13(5)
C11–H11...O2	3.031(1)	3.917(2)	159.95(5)

C1-H1...O1	2.562(1)	3.233(2)	129.45(5)
C5-H5...O1	2.610(2)	3.232(2)	124.72(5)
OW1-H1W1...N4	1.905(1)	2.778(1)	171.79(1)
N5-H5A...O4	2.132(1)	2.924(1)	154.52(1)
OW1-H2W1...O2	1.830(1)	2.663(1)	170.08(1)
OW2-H1W1...O3	1.968(1)	2.810(1)	171.56(5)
OW2-H2W2...O2	2.080(1)	2.937(1)	158.97(2)
N5-H5B...O8	2.127(2)	2.943(2)	154.53(1)
N6-H6B...O3	2.017(4)	2.884(4)	177.55(16)
N6-H6A...O2	2.597(2)	3.393(2)	161.38(20)

Table S4. Non-bonding and H-bonding interactions in complex **3**.

D-H...A	d(H...A) (Å)	d(D...A) (Å)	<DHA(°)
C12-H15...O4	2.675(1)	3.303(2)	125.58(5)
C7-H7...N2	3.031(4)	3.677(5)	158.07(20)
C16-H16C...O2	2.975(4)	3.860(5)	153.72(16)
N6-H6A...O1	2.057(4)	2.847(4)	158.45(5)
N6-H6B...O3	2.327(2)	2.832(1)	122.12(16)
N5-H5B...N3	2.470(1)	2.995(1)	122.52(20)
N5-H5A...O5	2.208(2)	2.994(2)	157.88(4)